A study of substitutional nitrogen impurities in chemical vapor deposited diamond

P. K. Sitch,[a] G. Jungnickel, M. Kaukonen, D. Porezag, and Th. Frauenheim
Theoretische Physik III, TU Chemnitz, D09107 Germany

M. R. Pederson and K. A. Jackson
Complex Systems Theory Branch, Naval Research Laboratory, Washington DC 20375

(Received 16 September 1997; accepted for publication 21 January 1998)

The behavior of substitutional N impurities in chemical vapor deposited diamond is examined theoretically in order to explain recent channeling experiments indicating a dominant onsite incorporation of N. The calculations are based on a combination of density-functional methods at various levels of approximation applied to supercell and cluster models. Neutral charge N impurities in the presence of highly defective carbon regions, such as dangling bonds, strained bonds, and partially developed π bonds are studied. We find a perfectly general argument concerning the position of the substitutional N atom in relation to the position of the Fermi level, E_f: if E_f lies above the A_1 level associated with the onsite substitutional N atom, off-site motion in the $\langle 111 \rangle$ direction is observed. Conversely, when E_f falls below A_1, N doping charge is transferred to the available deeper lying states. Suitable receptor states include surface dangling bonds, surface reconstruction π bonds, and bulk defects states such as grain boundaries and vacancies. © *1998 American Institute of Physics.* [S0021-8979(98)05509-1]

I. INTRODUCTION

The role of N in diamond continues to be of interest to the materials' scientist. Indeed, the failure to *n*-dope diamond and a number of recent experimental results[1–6] showing that the single substitutional nitrogen in chemical vapor deposited (CVD) diamond behaves rather differently than in natural diamond, have intensified this interest.

In natural and synthetic diamond, a variety of N-related defects have been identified and classified.[7] Foremost amongst these is the single substitutional N defect, which has been associated with a deep state 1.7 eV from the conduction band bottom and an electron-spin-resonance (ESR) signal at $g=2.0024$, labelled P_1. Various *ab initio* studies[7,8] have matched this to a neutral charge substitutional N sitting in a trigonally symmetric threefold coordinated arrangement, having been mutually repelled from one of its carbon atom neighbors along their $\langle 111 \rangle$ bonding axis.[7,8] The repelled C atom now has a dangling bond which pins the Fermi energy deep in the gap, with an additional filled state just above the valence band top associated primarily with the lone pair of electrons on the N atom. The physical mechanism for this off-site motion is now well understood and is due to the mutual repulsion of the lone pair of electrons on the N atom and a *p*-dangling bond on the neighboring C. A Jahn–Teller effect was previously thought responsible, but various theoretical workers have shown the ground state of the on-site N defect to be nondegenerate: of the three levels associated with the N atom, the singlet *s*-like state, A_1 lies lower in energy than the T_2 *p*-like doublet.[7,9,10] The P_1 defect is fourfold degenerate: N can move in any of four equivalent $\langle 111 \rangle$ directions, corresponding to breaking any one of the N–C bonds. Ammerlaan and Burgermeister[11] have lifted this degeneracy by applying uniaxial stress in a $\langle 111 \rangle$ direction. By annealing and fitting the resultant rate of N reorientation to a simple decay rule, they estimate the energy barrier between N equivalent off-site positions to be 0.7 eV. *Ab initio* calculations[12] confirm this value, noting the saddle point to be the on-site N position.

Over the past decade, much work has been carried out in investigating the effect of N on CVD diamond growth[13] and once incorporated, on how it affects the material's defect profile. Extensive effort has been made to completely characterize all defects found in N-doped CVD diamond.[1–6,14] ESR measurements[4] identify two signals, at $g=2.0024$ and 2.0029, respectively, the former being attributed to the P_1 center, as in natural diamond. The intensity of this line is strongly dependent on the N content, while the *g*-0029 signal is present in all samples. For samples with N concentration <15 ppm, the *g*-0024 signal occurs without having to illuminate the sample, whereas for $N>20$ ppm, it is only seen after illumination, with the increase in intensity equal to that of the increase from the $g=2.0029$ signal. This implies a charge transfer from a filled and hence passivated $g=2.0029$ level to an empty $g=2.0024$ state, rendering both ESR active. However, the percentage of N present thus activated constitutes only 1% of the total present in the material. The signal at $g=2.0029$, although attributable to C-related defects, increases in intensity proportionately with N incorporation. Rohrer *et al.*[1] relate this to a vacancy defect, whereas Zhou *et al.*[14] propose an H-vacancy complex. Zhou reasons that the four nearest neighbors to a C vacancy form two weak reconstruction bonds. When an H atom migrates into this defect, it breaks one reconstruction bond, forming a long C–H bond and leaving one C with a singly occupied

[a]Electronic mail:p.sitch@physik.tu-chemnitz.de

dangling bond, therefore being ESR. Electrostatic repulsion prevents further H atoms from entering the complex. This they have backed up by semiempirical AM1 and *ab initio* restricted open-shell Hartree–Fock (ROHF) cluster calculations. It is unclear, however, why the presence of N during growth promotes the formation of this defect. The observation of the g-0029 level at any N concentration and the increased density upon illumination reflects that the Fermi energy is pinned at the related defect level, rendering it partially filled and providing a reservoir for further ESR activation of g-0029 levels.

Constant-photocurrent methods (CPM), which map accurately bulk defect states, record two principal states associated with N content: a level at 1.6 eV below the conduction band, attributable to substitutional diamond and a level 1.0 eV above the valence band, which they identify with the $g=2.0029$ signal. In contrast, photothermal deflection spectroscopy (PDS) measurements, which detect spatially resolved spectral states and are sensitive to absorption by surface states, detect a high concentration of active band gap states on the surface or in grain boundaries,[1] which they identify to be π^* in nature. These states lie in a broad band up to 2 eV below the conduction band bottom. Nebel[15] suggests that a Schottky barrier situation exists between such surfacelike states and the bulk crystal, allowing the Fermi level in the crystallites to be different to that in the grain boundary and surface regions. In this way, there is no contradiction in the fact that the Fermi level in bulk and grain boundaries lies at different positions in the band gap.

In this article, we explain the fourfold coordinated nature of N in CVD diamond. We draw on previous density functional tight-binding (DF-TB) studies of N in diamond and tetrahedral amorphous carbon (ta-C),[16] as well as modeling theoretically the effect of N below reconstructed and partially passivated (100) and (111) surfaces, in the neutral charge state and the charged N defect in bulk. The subsurface configurations mimic the incorporation of N in CVD diamond in situations in which highly defective carbon regions with dangling bonds, strained bonds, or partially developed π bonds are present. Although these calculations can explain directly only the PDS results, we use Fermi level arguments to show that the results can be applied to explain the general behavior of N in CVD diamond. The article is arranged as follows, in Sec. II the theoretical tools used in this study are described, while Sec. III contains results for the (111) and (100) surfaces. Finally, Sec. IV comprises a discussion and a brief conclusion.

II. THEORETICAL METHOD

The density functional tight-binding method (DF-TB)[17] derives its name from its use of self-consistent density functional calculations for pseudoatoms in order to construct transferable tight-binding (TB) potentials for a nonself-consistent solution of the Kohn–Sham equations for the many body case. It differs from conventional tight-binding techniques, in that there is a systematic way of deriving these potentials, independent of the atom type involved. This is thus not a ''parametrization'' as is usually meant when one talks about TB approaches. For an in depth description, the reader is referred to Ref. 18. The method has been successfully applied to all-scale carbon systems, ranging from small clusters to buckminster fullerenes and the bulk phase,[18] the electronic and vibrational properties of (100) and (111) surfaces,[19,20] amorphous carbon systems of all densities,[21] as well as boron nitride[22] and boron and nitrogen doping of diamond and amorphous systems.[16] We have also checked selected results by using the all-electron *ab initio* cluster program developed by two of the co-workers (M.R.P. & K.A.J.).[23]

The 132 atom (111) supercell used in this investigation comprises 10 layers and 12 surface C atoms, whilst the 224 atom (100) supercell is made up of 8 reconstructed surface bonds and 12 layers of carbon atoms. In both cases, the dangling bonds on the lower surface are terminated with pseudohydrogen atoms. Unless otherwise stated, we have performed conjugate gradient relaxations, keeping the pseudohydrogen atoms and the lowest two layers of C atoms fixed.

III. RESULTS

A. The (111) surface

We take the relaxed Pandey chain reconstructed clean (111) surface reported in earlier DF-TB studies,[14] with C–C surface chain bond lengths of 1.44 Å and slightly compressed bonds to subsurface atoms of length 1.52 Å. Inspection of the total electronic density of states (TDOS) shown in Fig. 1(a) clearly reveals how the surface reconstruction π bonding has introduced a fully occupied π shoulder into the bulk diamond σ band edge, the highest occupied molecular orbital (HOMO) being indicated by E_1, and an empty set of π^* states into the lower half of the bulk diamond $\sigma-\sigma^*$ band gap. Here the lowest unoccupied molecular orbital (LUMO) is represented by E_2. Relaxation of the supercell with a substitutional nitrogen impurity in the fourth layer below the surface produces a minimum energy structure in which the N atom sits on-site in a fourfold coordinated arrangement with C–N bonds of lengths 1.54 and 1.50 ($x3$). A Mulliken charge analysis shows the migration of an electron from the N atom environment to the surface, where it is accommodated in an antibonding π^* state. This surface state is delocalized along one of the Pandey chains, causing a lengthening of the chain bonds from 1.44 to 1.48 Å. The electronic TDOS for the supercell in Fig. 1(a), reveals the Fermi energy (E_4) to be pinned by this partially occupied π^* state just below midgap. The highest energy state occupied by the N atom is indicated by E_3 in the diagram, and can clearly be seen to lie somewhat lower in energy than the E_f. This is the same effect as that which we have reported[16] for N impurities in ta-C, where we see a transfer of charge from the N environment to a π^* state, resulting in the Fermi energy being pinned by a strongly localized midgap state, preventing any shallow doping.

In order to check that our configuration is in fact the minimum energy one, we moved the N atom off site in various directions up to a distance of 0.3 Å, with the result that the N atom always returns to the above described position. We have also repeated calculations at various alternative

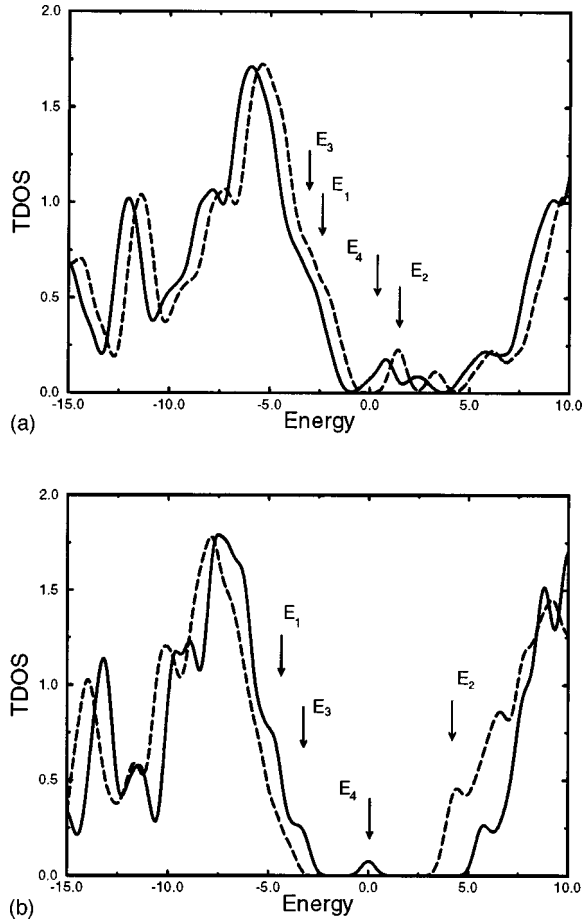

FIG. 1. Total density of states for (a) the unhydrogenated and (b) hydrogenated (111) surface structures, respectively: straight line with subsurface N, dotted line without. E_1 and E_2 are the HOMO and LUMO for the surface without N, E_3, and E_4 are the highest energy state associated with N and E_f, respectively. In both cases, the position of the E_f is normalized to zero energy.

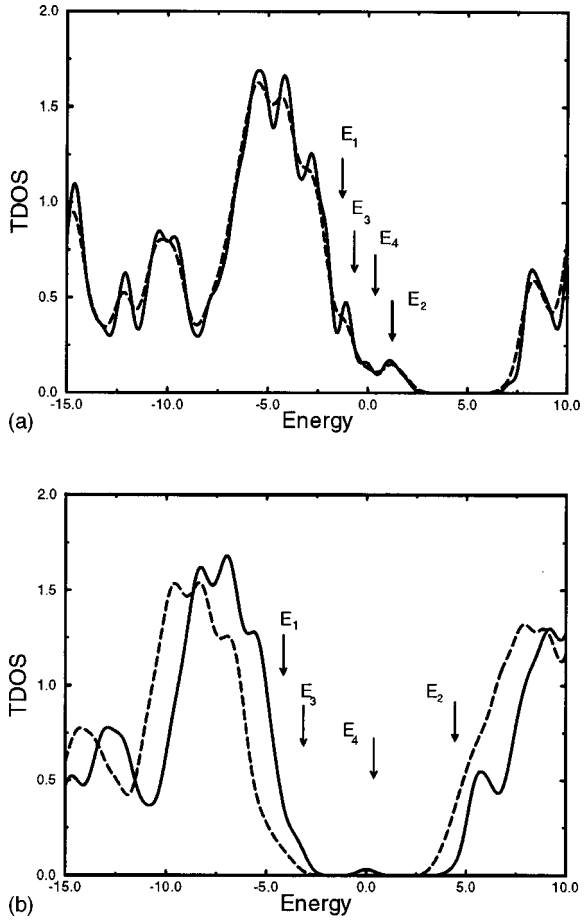

FIG. 2. Total density of states for (a) the unhydrogenated and (b) hydrogenated (100) surface structures, respectively: straight line with subsurface N, dotted line without. E_1 and E_2 are the HOMO and LUMO for the surface without N, E_3, and E_4 are the highest energy state associated with N and E_f, respectively. In both cases, the position of the E_f is normalized to zero energy.

substitutional sites within the layer and also in other subsurface layers. We observe no deviation from the physics described above: the N stays on-site, with this process stabilized by the transfer of charge to an antibonding surface state, resulting in Fermi level pinning.

For our investigation of the hydrogenated surface, we have chosen to use the (1×1) symmetry, as this was found previously to be lower in energy than the hydrogenated Pandey chain.[24] We observe in Fig. 1(b) how the removal of the C–C surface π bonds via the formation of C–H bonds of length 1.12 Å clears the $\sigma-\sigma^*$ band gap of surface states. Here the HOMO and LUMO are indicated by E_1 and E_2, respectively. We recover for the case of substitutional subsurface N the results found in bulk diamond for the neutral defect: the N atom moves off-site, breaking one of its C–N bonds and sitting threefold coordinated with three C–N bonds of length 1.45 Å. E_f is pinned by a midgap partially filled state localized on the neighboring threefold coordinated carbon atom, with the highest energy state associated with N lying just above the valence band top [E_4 and E_3, respectively, in Fig. 1(b)].

In order to study the partially hydrogenated case, we remove a single H atom from the (111): H surface. This introduces a partially filled midgap dangling bond surface level and results in a spontaneous onsite motion of the N atom and the migration of one electron to this newly available surface state.

B. The (100) surface

The clean π bonded (2×1) chain (100) surface found by DF-TB and various existing theoretical[22,25,26] and experimental[27] studies to be most stable is used in this study. The surface carbon atoms have two σ bonds to subsurface carbon atoms of lengths 1.52 Å and one surface π bond of length 1.39 Å. As in the (111) surface case, this reconstruction leads to an occupied π shoulder of states at the diamond σ band edge, the highest energy of which is indicated by E_1, and an unoccupied π^* band of states in the lower half of the band gap, the lowest energy of which indicated by E_2, [see Fig. 2(a)]. A subsurface substitutional nitrogen atom placed four layers below the surface behaves identically to that of the (111) case, remaining fourfold coordinated with bond lengths 1.49, 1.49, 1.47, and 1.51 Å, returning to this arrangement even when moved off-site by hand by a distance of 0.3 Å and subsequently rerelaxed. Mulliken charge studies

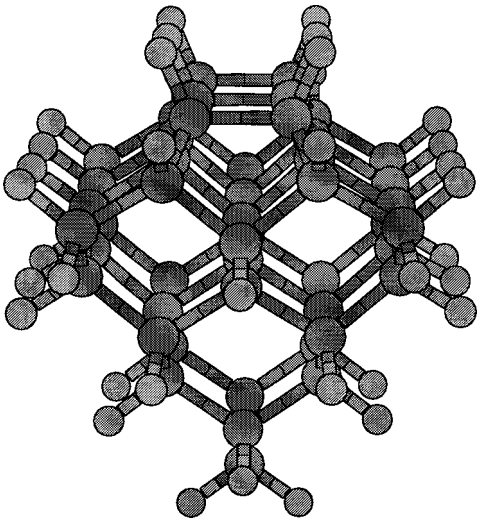

FIG. 3. The 88 atom cluster simulating the partially covered (100) H surface. The top six carbon atoms represents the surface, the middle two of which are not hydrogenated and are π bonded to each other.

show that an electron migrates from the N impurity atom to the surface, where it sits in an antibonding π^* state [E_4 in Fig. 2(a)] localized along one of the reconstruction chains, pinning the Fermi energy 0.72 eV above the π-valence band top in the process. The C–C chain bonds lengthen from 1.38 to 1.41 Å as a result. Again the highest energy state associated with the N atom lies well below E_f and is indicated by E_3 in Fig. 2(a). As for the (111) surface, the fourfold N geometry is also stable for the partially hydrogenated (100) surface, since the partially filled/empty gap states associated with the surface are thence not fully removed and can act as sinks for N ''doping'' charge. For the fully hydrogenated surface, we recover exactly the same results as for the (111) surface: hydrogenating the surface clears the $\sigma-\sigma^*$ band gap of states. On placing a substitutional N atom four layers below the surface the N atom moves to the threefold coordinated position, with E_f pinned deep in the gap [E_4 in Fig. 2(b)] by an electron located on a C atom neighboring the N.

C. Self-consistent field results

We demonstrate the authenticity of our DF-TB results by undertaking similar calculations using two different self-consistent field (SCF) *ab initio* cluster programs: the all electron SCF method of Pederson and Jackson[23] and the pseudopotential code AIMPRO of Jones and Briddon.[28] A small cluster was extracted from a large (100) supercell and the bulk dangling bonds saturated with hydrogen atoms (Fig. 3). The uppermost six carbon atoms represent the (100) surface, the outer two pairs of C atoms having H-terminating bonds, whilst the inner two C atoms form a reconstructed π bond of length 1.38 Å. Structural relaxation is undertaken within AIMPRO and DF-TB. For the all electron method this would have been computationally prohibitive—we have instead compared the energies of the fourfold coordinated onsite structure and the threefold coordinated offsite structure (both prerelaxed using DF-TB). Our results are summarized in Table I, where it can be seen that all methods agree that the fourfold arrangement is energetically favored, with DF-TB and AIMPRO finding a spontaneous on-site relaxation of the off-site N atom.

TABLE I. Energetic ordering of the single N defect configurations for DF-TB, all electron SCF, and AIMPRO in the case where E_f is pinned below the N on-site A_1 level.

	DF-TB	All electron	AIMPRO
On-site energy (eV)	0.0	0.0	0.0
Off-site energy (eV)	1.90 (unstable)	1.40	0.62 (unstable)
N–C onsite bond length (Å)	1.53	1.53	1.55
C–C unhydrogenated surface dimer bond length (Å)	1.47	1.47	1.49

If the surface π bond is broken by hydrogenating one of the carbon atoms (giving an 89 atom cluster), we also recover within AIMPRO and DF-TB exactly the same physics as described above—an onsite stabilization of the N atom, with the electron then moving to a surface lone pair site. Computational cost prevented us from repeating this calculation with the all-electron method. The predicted gain is 1.1 and 1.4 eV within AIMPRO and DF-TB respectively for the spontaneous on-site motion of the N atom.

We thus have SCF agreement for the main physical model underlying our results: when π^* surface states are present at a surface, a subsurface N atom can stabilize a fourfold coordinated site by transferring its' doping charge into this state.

IV. DISCUSSIONS AND CONCLUSIONS

Theoretically we have studied the position of N atoms below diamond surfaces, showing that, although the off-site threefold coordinated N is more stable than a substitutional on-site fourfold arrangement in the bulklike diamond (i.e., where the $\sigma-\sigma^*$ bulk band gap is clear of states), in systems where dangling bonds or π^* antibonding states are present in the band gap, the fourfold coordinated on-site N arrangement is stabilized by a charge transfer from the N environment to these deeper lying states. It is instructive to couch the discussion in terms of Fermi level arguments: in the neutral charge state, the fourfold coordinated N is unstable with respect to off center $\langle 111 \rangle$ distortions due to an excess of local charge. As a consequence, the HOMO, the singly occupied A_1 level, is driven deep into the gap, the energy cost of distorting the stiff diamond lattice being off-set by a lowering in the electrostatic energy. When the Fermi level is pinned by a state lower in the band gap than the (on-site) A_1 state, A_1 is empty, no local charge excess around the N impurity exists, no off-site motion takes place and therefore the (charge+1) N defect sits fourfold coordinated and on-site. We have checked the behavior of the charge+1 N defect using a 216 atom supercell and find that the on-site N is indeed lower in energy, with the empty A_1 level lying 0.8 eV from the conduction band bottom. Street[29] has previously used such arguments to explain the on-site position of phosphorus in amorphous silicon.

We can understand the experimental work in the light of these findings. The initial absence of the P_1 state (associated with the off-site substitutional N) in ESR measurements for CVD bulk material, and its activation via a charge transfer from $g=2.0029$ during illumination implies E_f to be pinned below the N A_1 level. Since the $g=2.0029$ is seen without illumination, some of the associated states must be partially filled, hence the band gap is pinned within the broad band of $g=2.0029$ states, lying ≈ 1 eV above the valence band top. At the surface or in grain boundaries, E_f is pinned by π^*, which as we have seen in this article are also suitable sinks for N doping charge. Thus in both cases, the N atom is passivated and sits on-site in the CVD diamond lattice. In a previous article describing N effects in tetrahedral amorphous carbon,[16] we argued that the passivation of N defects by localized π^* states was consistent with the n- type nature of the material, since the dominant carriers were still electrons and the relevant conduction mechanism is now hopping between the π^* defect clusters. We predict this to be the case in CVD diamond, with the hopping occurring between π^* grain boundary and/or surface states.

Our model suggests therefore that current CVD growth techniques, which result in diamond with high densities of intrinsic defects, necessarily lead to N-doped samples where the $g=2.0024$ state is not observed in ESR experiments. In the absence of better CVD samples, we can only suggest by way of an experimental test of our hypothesis the connection of the grown CVD sample to an ohmic cathodic contact. The resultant supply of electrons will shift the Fermi level of the sample towards the conduction band. According to our model, this will result in the motion of subsurface N atoms from four to threefold, whence the $g=2.0024$ state should start to be observed in an ESR experiment (provided the nature of the π bonded regions does not change in this process).

To summarize, the difference in behavior of N in diamond and CVD diamond can thus be regarded as being due to the presence in CVD diamond of a greater density of intrinsic defects, such as grain boundaries, dislocations, and vacancies, which pin E_f deep in the gap, acting as sinks for the excess N doping charge, enabling N to remain fourfold coordinated. Since the doping charge is now resident in deep lying, localized states, no doping is implied.

ACKNOWLEDGMENT

The support of the Deutsche Forschungsgemeinshaft is gratefully acknowledged.

[1] E. Rohrer, C. F. O. Graeff, R. Janssen, C. E. Nebel, M. Stutzmann, H. Güttler, and R. Zachai, Phys. Rev. B **54**, 7874 (1996).
[2] R. Samlenski, C. Haug, R. Brenn, C. Wild, R. Locher, and P. Koidl, Diamond Relat. Mater. **67**, 947 (1996).
[3] E. Rohrer, C. F. O. Graeff, C. E. Nebel, M. Stutzmann, H. Güttler, and R. Zachai, Mater. Sci. Eng., B **46**, 115 (1997).
[4] C. F. O. Graeff, E. Rohrer, C. E. Nebel, M. Stutzmann, H. Güttler, and R. Zachai, Appl. Phys. Lett. **69**, 3215 (1996).
[5] C. F. O. Graeff, E. Rohrer, C. E. Nebel, M. Stutzmann, H. Güttler, and R. Zachai, Mater. Res. Soc. Symp. Proc. **423**, 495 (1996).
[6] C. E. Nebel, J. Münz, M. Stutzmann, R. Zachai, and H. Güttler, Phys. Rev. B **55**, 1 (1997).
[7] P. R. Briddon and R. Jones, Physica B **185**, 179 (1993).
[8] S. A. Kajihara, A. Antonelli, and J. Bernholc, Physica B **185**, 144 (1993).
[9] G. B. Bachelet, G. A. Baraff, and M. Schlüter, Phys. Rev. B **24**, 4736 (1981).
[10] K. Jackson, M. R. Pederson, and J. Harrison, Phys. Rev. B **41**, 12 641 (1990).
[11] C. A. J. Ammerlaan and E. A. Burgermeister, Phys. Rev. Lett. **47**, 954 (1987).
[12] S. J. Breuer and P. R. Briddon, Phys. Rev. B **53**, 7819 (1996).
[13] R. Locher, C. Wild, N. Herres, D. Behr, and P. Koidl, Appl. Phys. Lett. **65**, 34 (1994).
[14] X. Zhou, G. D. Watkins, K. M. McNamara-Rutledge, P. Messmer, and S. Chawla, Phys. Rev. B **54**, 7881 (1996).
[15] C. E. Nebel (private communication).
[16] P. K. Sitch, Th. Köhler, G. Jungnickel, D. Porezag, and Th. Frauenheim, Solid State Commun. **100**, 549 (1996).
[17] G. Seifert and H. Eschrig, Phys. Status Solidi B **127**, 573 (1985).
[18] D. Porezag, Th. Frauenheim, Th. Köhler, G. Seifert, and R. Kaschner, Phys. Rev. B **51**, 12 947 (1995).
[19] Th. Köhler, M. Sternberg, D. Porezag, and Th. Frauenheim, Phys. Status Solidi A **154**, 69 (1996).
[20] Th. Frauenheim, Th. Köhler, M. Sternberg, D. Porezag, and M. R. Pederson, Thin Solid Films **272**, 314 (1996).
[21] U. Stephan, Th. Frauenheim, P. Blaudeck, and G. Jungnickel, Phys. Rev. B **50**, 1489 (1994).
[22] J. Widany, Th. Frauenheim, Th. Köhler, M. Sternberg, G. Jungnickel, and G. Seifert, Phys. Rev. B **53**, 4443 (1995).
[23] M. R. Pederson and K. A. Jackson, Phys. Rev. B **43**, 7312 (1991).
[24] Th. Frauenheim, U. Stephan, P. Blaudeck, D. Porezag, H. G. Bussmann, W. Zimmermann-Edling, and S. Lauer, Phys. Rev. B **48**, 18 189 (1993).
[25] D. R. Alfonso, D. A. Drabold, and S. E. Ulloa, Phys. Rev. B **51**, 14 669 (1995).
[26] Th. Frauenheim, U. Stephan, P. Blaudeck, D. Porezag, H. G. Busmann, W. Zimmermann-Edling, and S. Lauer, Phys. Rev. B **48**, 18 189 (1993).
[27] J. Weide, Z. Zhang, P. K. Baumann, M. G. Wensell, J. Bernholc, and R. J. Nemanich, Phys. Rev. B **50**, 5803 (1994).
[28] R. Jones, Philos. Trans. R. Soc. London, Ser. A **341**, 157 (1992).
[29] R. A. Street, Phys. Rev. Lett. **49**, 1187 (1982).